Error Performance of a Pulse Amplitude and Position Modulated Ultra-Wideband System Over Lognormal Fading Channels

Huaping Liu, *Member, IEEE*

***Abstract*—In this letter, the error performance of an ultra-wideband (UWB) system with a hybrid pulse amplitude and position modulation (PAPM) scheme over indoor lognormal fading channels is analyzed. In the PAPM UWB system, input data is modulated onto both the pulse amplitudes and pulse positions. The receiver employs a RAKE to combine energy contained in the resolvable multipath components. Derivation of closed-form error rate expressions of the system in lognormal fading channels is based on approximating a sum of independent lognormal random variables (RVs) as another lognormal RV using the Wilkinson's method. Given the same delay spread of the channel, the proposed PAPM scheme can provide a higher throughput than the binary pulse amplitude or pulse position modulation scheme.**

***Index Terms*—Lognormal fading, performance analysis, ultra-wideband (UWB).**

I. Introduction

ULTRA-WIDEBAND (UWB) communications [1] has recently attracted significant academic and commercial interest mainly because of its high-data-rate capabilities over short distances. Achievable data rates of practical UWB systems, however, are limited by the minimum pulse repetition interval determined by the maximum acceptable inter-symbol interference level. The commonly used UWB signals which employ the pulse position modulation (PPM) scheme exhibit spectral lines [2]. Because UWB systems use spectrum that might be occupied by existing narrowband systems, generating UWB signals with a flat power spectral density (no spectral lines) is of great importance to minimize interference to the overlaying narrowband systems. It was shown in [2] that systems employing the hybrid pulse amplitude and position modulation (PAPM) scheme do not have spectral lines. Another advantage of the hybrid modulation scheme is that it has the potential to double the throughput of a binary pulse amplitude or position modulation system.

In this letter, we propose a new PAPM UWB receiver and analyze its error performance over lognormal fading channels. We use a RAKE receiver to combine the energy contained in a subset of the resolvable multipath components and derive the closed-form error rate expressions.

Manuscript received April 2, 2003. The associate editor coordinating the review of this paper and approving it for publication was Prof. Z. Xu.

The author is with the Department of Electrical Engineering and Computer Science, Oregon State University, Corvallis, OR 97331 USA (e-mail: hliu@eecs.orst.edu).

Digital Object Identifier 10.1109/LCOMM.2003.820079

II. System Model

In the PAPM UWB system, the nth transmitted symbol is represented by two bits as $a_n = [b_n^0, b_n^1]$. These bits are converted into the nonreturn-to-zero form, i.e., $b_n^0, b_n^1 \in \{\pm 1\}$ and $a_n \in \{11,\ 1-1,\ -11,\ -1-1\}$. The symbol sequence is precoded by interchanging the two symbols $\{-11\}$ and $\{-1-1\}$. The transmitted UWB signal is expressed as

$$s(t) = \sum_{n=-\infty}^{\infty} \sqrt{E_s} b_n^0 p\left(t - nT_s - \frac{1-b_n^1}{2}\Delta\right) \quad (1)$$

where E_s is the symbol energy, T_s is the symbol interval (much greater than the pulse duration), and $p(t)$ is the short-duration UWB pulse shape (e.g., a windowed Gaussian monopulse) whose energy is normalized to $E_p = \int_{-\infty}^{\infty} p^2(t)dt = 1$. If the incoming bit b_n^0 is l, a positive pulse is sent. Otherwise a negative pulse is sent. If the incoming bit b_n^1 is -1, the pulse is shifted relative to the time reference by Δ. There is no time shift if the incoming bit b_n^1 is 1.

The impulse response of the channel can be modeled as [3]

$$h(t) = \sum_{l=0}^{L-1} \alpha_l \delta(t - l\mathcal{T}_p) \quad (2)$$

where L is the number of resolvable multipath components, $\mathcal{T}_p$ is the minimum multipath resolution, $\delta(t)$ is the Dirac delta function, and $\alpha_l = \theta_l \beta_l$ is the fading coefficient of the l^{th} resolvable path. The parameter $\theta_l \in \{\pm 1\}$ with equal probability is used to account for the random pulse inversion that can occur due to reflections [3] and β_l represents the fading amplitude. Given the short-duration pulse shape $p(t)$, the multipath resolution $\mathcal{T}_p$ is equal to the pulsewidth of $p(t)$.

It has been concluded in [4], [5] that for most indoor channels the fading amplitude is lognormally distributed with a standard deviation of 3–5 dB. Thus β_l has lognormal fading statistics and is considered to be constant during a symbol interval. The received signal can be written as

$$r(t) = \sum_{l=0}^{L-1} \alpha_l s(t - l\mathcal{T}_p) + n(t) \quad (3)$$

where $n(t)$ is the additive white Gaussian noise (AWGN) process with a two-sided power spectral density of $N_0/2$.

The PAPM UWB receiver structure is shown in Fig. 1. The received signal is correlated by using two template waveforms

$$\phi_1(t) = p(t) + p(t - \Delta) \quad (4a)$$

$$\phi_2(t) = p(t) - p(t - \Delta) \quad (4b)$$

where Δ was defined in (1). The correlator output is integrated and then combined using maximal ratio combining. Decisions

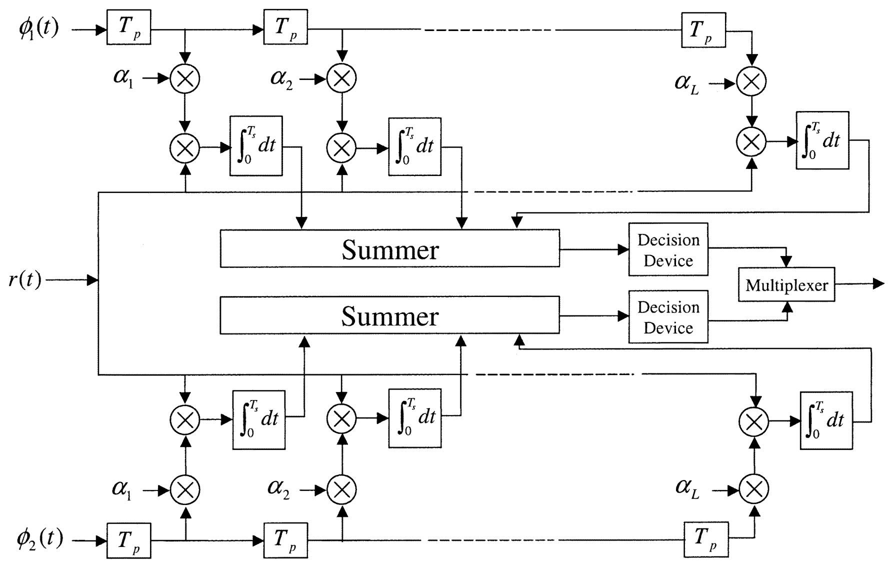

Fig. 1. A RAKE receiver for the PAPM UWB system.

are made independently for each correlator output and then multiplexed, forming the estimate of the transmitted symbols.

III. Performance Analysis

We derive the bit error rate (BER) of this receiver. With independent input bits, the symbol error rate (SER) can be easily calculated using the BER. The pulse shape $p(t)$ is assumed to be obtained by windowing a Gaussian monopulse $g(t;\tau) = (t/\tau^2)exp[-2\pi(t^2/2\tau^2)]$. Performance of the proposed receiver depends on the choice of values for Δ. In this letter, the orthogonal signaling [6] scheme is adopted. In this scheme, Δ is chosen to be the minimum value such that $\int_{-\infty}^{\infty} p(t)p(t-\Delta)dt = 0$. Depending on the width of $p(t)$, Δ for orthogonal signaling is a fraction of the pulse duration and $\int_{-\infty}^{\infty} p(t-\Delta)p(t-\mathcal{T}_p)dt \approx 0$. It is also assumed that perfect estimates of fading coefficients (α_l) of each path are available at the receiver.

Without loss of generality, we focus on the detection of the first symbol. The decision variables are expressed as

$$\lambda_i = \sum_{l=0}^{L-1} \alpha_l \int_0^{T_s} r(t)\phi_i(t - l\mathcal{T}_p)dt, \qquad i = 1, 2 \tag{5}$$

where $\phi_1(t)$ and $\phi_2(t)$ are the template waveforms applied. Due to the orthogonality between $\phi_1(t)$ and $\phi_2(t)$, the Gaussian noise components at the output of the two correlators for the l^{th} path can be easily shown to be independent from each other. Thus, symbol decisions can be made by passing λ_1 and λ_2 independently through a decision device of threshold zero. The precoding scheme described in Section II ensures that the decisions based on λ_1 and λ_2 correspond, respectively, to bits b_n^0 and b_n^1 before the precoding. Because decisions for bits b_n^0 and b_n^1 of each symbol can be made independently, the bit error rate can be analyzed based on the statistics of either λ_1 or λ_2.

For a fixed set of fading coefficients $\{\alpha_l\}$, λ_i is a Gaussian random variable (RV). Because the energy of $p(t)$ is normalized to unity, the instantaneous signal-to-noise ratio (SNR) per bit, γ_b, is obtained as

$$\gamma_b = \frac{E_s}{N_0} \sum_{l=0}^{L-1} \alpha_l^2 = \sum_{l=0}^{L-1} \gamma_l \tag{6}$$

where $\gamma_l = (E_s/N_0)\beta_l^2$ ($\alpha_l = \theta_l\beta_l$ and $\theta_l \in \{\pm\}$). Because β_l is a lognormal RV, $\gamma_l = (E_s/N_0)\beta_l^2$ is also a lognormal RV. Thus, γ_b is a sum of independent lognormal RVs β_l, $l = 0, \cdots, L-1$.

As in [7], we calculate the BER for a fixed set of $\{\beta_l\}$ and then average the conditional BER over the probability density function (PDF) of γ_b. The conditional BER for a fixed set of $\{\beta_l\}$ is given as

$$p(\gamma_b) = \frac{1}{2}\text{erfc}\left(\sqrt{\frac{\gamma_b}{2}}\right). \tag{7}$$

Let $\beta_l = e^{y_l}$ where y_l is a normal RV, i.e., $y_l \sim N(\mu_{y_l}, \sigma_{y_l}^2)$. Then

$$\gamma_l = e^{c_0 + 2y_l} \tag{8}$$

where $c_0 = \ln(E_s/N_0)$. The kth moment of β_l is given as

$$E\left\{\beta_l^k\right\} = e^{\frac{k\mu_{y_l} + k^2\sigma_{y_l}^2}{2}}. \tag{9}$$

Although an exact closed-form expression for the PDF of a sum of independent lognormal RV's does not exist, such a sum can be approximated by another lognormal RV [8]. The approximation can be obtained by a number of methods, one of which is the Wilkinson's method [8].

Let $\gamma_b = e^z$ where z, $z \sim N(\mu_z, \sigma_z^2)$, is a normal RV. In Wilkinson's method, the two parameters μ_z and σ_z are obtained by matching the first two moments of γ_b with the first two moments of $\sum_{l=0}^{L-1} \gamma_l$. These two parameters are given as

$$\mu_z = \ln\left(\frac{E_{L1}^2}{\sqrt{E_{L2}}}\right) \tag{10a}$$

$$\sigma_z = \ln\left(\frac{E_{L2}}{E_{L1}^2}\right) \tag{10b}$$

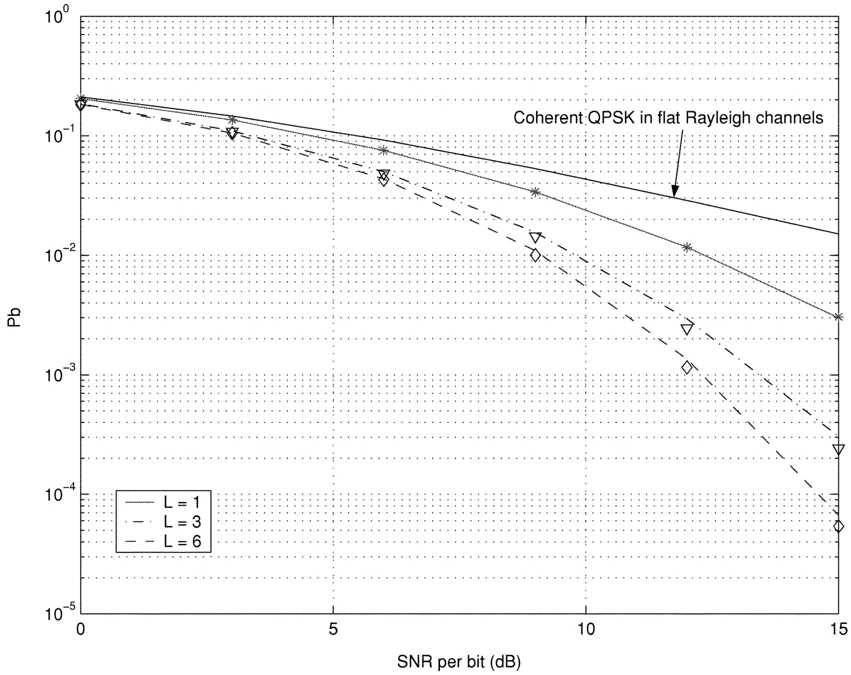

Fig. 2. Analytical and simulated (with marks) error performance curves.

where E_{L1} and E_{L2} are related to μ_{y_l} and $\sigma_{y_l}^2$ as

$$E_{L1} = \sum_{l=0}^{L-1} e^{\left(c_0 + 2\mu_{y_l} + 2\sigma_{y_l}^2\right)} \tag{11a}$$

$$E_{L2} = \sum_{l=0}^{L-1} e^{2\left(c_0 + 2\mu_{y_l} + 4\sigma_{y_l}^2\right)} + 2\sum e^{2\left(c_0 + \mu_{y_m} + \mu_{y_n} + \sigma_{y_m}^2 + \sigma_{y_n}^2\right)} \tag{11b}$$

where the second sum in (11b) is extended to all combinations of (m, n), $m < n = 0, \cdots, L-1$.

The approximated PDF of γ_b is given as

$$f(\gamma_b) = \frac{1}{\gamma_b\sqrt{2\pi\sigma_z^2}} \exp\left[-\frac{(\ln(\gamma_b) - \mu_z)^2}{2\sigma_z^2}\right]. \tag{12}$$

The average BER can be calculated by averaging the conditional BER $p(\gamma_b)$ over $f(\gamma_b)$ as

$$P_b = \int_0^\infty p(\gamma_b) f(\gamma_b) d\gamma_b. \tag{13}$$

IV. Numerical Results and Discussion

In the numerical examples, an exponential power decaying profile [5] with the power of the first path ($l = 0$) normalized (i.e., $E\{\alpha_l^2\} = e^{-\rho l}$) and $\rho = 0.046$ is adopted. Typical values of the standard deviation of fading coefficients β_l for indoor channels fall in the range of 3–5 dB [4]. For this range of values, the Wilkinson's method provides accurate approximation to the PDF of γ_b. For a 4-dB standard deviation of β_l, σ_{y_l} is calculated to be $\sigma_{y_l} = 0.46$ dB. Although the number of resolvable multipath components is typically very large for UWB channels, combining a large number of paths becomes too complex and therefore impractical. The analytical and simulated (with marks) curves of BER versus the average SNR per bit defined as $\overline{\gamma}_b = (E_s/N_0)\sum_{l=0}^{L-1} e^{-\rho l}$ are shown in Fig. 2. Curves shown are for cases when $L = 1$, 2, and 6 resolvable multipath components are combined by the RAKE. The analytical results based on approximating the PDF of γ_b and the simulated results (with marks) match well. For comparison purposes, the error rate curve for coherent quadriphase-shift keying ($E_s = 2E_b$ is used in calculating $\overline{\gamma}_b$) in a Rayleigh flat-fading ($L = 1$) channel is also provided in Fig. 2. It is found that the error performance of the PAPM UWB system in lognormal fading channels with $L = 1$ is better than that of coherent quadriphase-shift keying in flat Rayleigh fading channels.

V. Conclusion

A UWB system which employs a hybrid pulse amplitude and position modulation scheme is proposed. The proposed system does not exhibit spectral lines and has the potential to double the throughput of a binary PAM or PPM system. Analytical error rate expressions of this system over lognormal fading channels are derived.

References

[1] M. Z. Win and R. A. Scholtz, "Impulse radio: how it works," *IEEE Commun. Lett.*, vol. 2, pp. 36–38, Feb. 1998.
[2] Y. Li and X. Huang, "The spectral evaluation and comparison for ultra-wideband signals with different modulation schemes," in *Proc. 2000 World Multiconf. on Systemics, Cybernetics and Informatics (SCI 2000)*, vol. VI, July 2000, pp. 277–282.
[3] *UWB Channel Modeling Contribution From Intel*, IEEE P802.15-02/279-SG3a.
[4] H. Hashemi, "The indoor radio propagation channel," *Proc. IEEE*, vol. 81, pp. 943–967, July 1993.
[5] J. R. Foerster, "The effects of multipath interference on the performance of UWB systems in an indoor wireless channel," in *Proc. 53rd IEEE VTC (Spring)*, vol. 2, 2001, pp. 1176–1180.
[6] R. Scholtz, "Multiple access with time-hopping impulse modulation," in *Proc. MILCOM'93*, vol. 2, 1993, pp. 447–450.
[7] J. G. Proakis, *Digital Communications*, 3rd ed. New York: McGraw-Hill, 1995, ch. 14.
[8] N. C. Beaulieu, A. A. Abu-Dayya, and P. J. Mclane, "Estimating the distribution of a sum of independent lognormal random variable," *IEEE Trans. Commun.*, vol. 43, pp. 2869–2873, Dec. 1995.